

Shielding Effectiveness Evaluation of Enclosure with Apertures Using Electro-Optic Sensor

No-Weon Kang, Dong-Joon Lee

Center for Electromagnetic Wave
Korea Research Institute of Standards and Science
Daejeon, Korea
{nwkang, dongjoonlee}@kriss.re.kr

Wonjune Kang, Youngseek Chung

Department of Wireless Communication Engineering
Kwangwoon University
Seoul, Korea
Astin1983@naver.com, yschung@kw.ac.kr

Abstract—Shielding effective (SE) evaluations inside multiple cavities consisted of various coupling paths have been presented. Modeling based on electromagnetic topology (EMT) is performed to solve the problem fast and efficiently. A minimally invasive electric field measurement system by using an electro-optic sensor which can minimize the invasiveness of internal field is proposed. Results given by simulations are experimentally validated showing good agreement.

Keywords—fiber optic sensor; microwave photonics; electro-optics; electromagnetic topology;

I. INTRODUCTION

Metallic enclosures to protect electronic equipment are widely used to cope with electromagnetic interferences (EMIs), which can lead to malfunction or even destruction of the system [1], [2]. However the external fields can be penetrated to the systems have various paths such as antennas, power or data lines, apertures or slits on the enclosures. As a measure of the protection SE (shield effectiveness) has always been an important subject of interest in electromagnetics.

To predict the SE of the system one of the most popular methods is numerical analysis based on mature computational techniques. However such simulation methods for large structures usually require many hours or even days of computing time. Therefore the method based on EMT (Electromagnetic Topology) is applied to the large and complicated structures for its fast speed of solving compared to other full-wave analysis methods. This EMT analysis method introduced by Baum involves dividing large entire structure into sub-volumes with proper characterizing and reconstructing the whole system as the topology [3], [4].

The measurement of the fields inside a small and complicated system has been a challenging task due to the invasiveness of the field sensor itself. Normally commercial field sensors are not compact enough to fit inside the shielding enclosures that have small volume. Therefore the short dipole or monopole antennas are employed for its small size [5]. However, these metallic antennas also change the internal fields inside the system due to their invasiveness, and they are hard to be accessible for various positions inside the system because of their lengthy and wired structures.

Fiber based electro-optic (EO) sensor has garnered much attention due to its wide frequency range and minimal invasiveness compared to metallic probes [6], [7]. This is because the probe geometry and its all-dielectric embodiment are fairly transparent to not only the optical beam but also microwave frequency fields.

In this paper, field analysis inside multiple cavities is studied by using an EMT approach and microwave photonic measurement system. Modeling based on EMT is will be discussed. Then the description of the metallic cavities for shielding effectiveness (SE) analysis and the numerical field simulation of the cavity are followed. For experimental verification the configuration of the sensing system associated with the EO (Electro-Optic) sensor is described. Experimental results of EO sensor are given in Section II-B.

II. FIELD ANALYSIS INSIDE THE MULTIPLE CAVITIES

As a typical model of multiple cavities, we considered a simplified vehicle that is made of aluminum with dimensions of 165 mm (x) \times 142.5 mm (y) \times 100 mm (z) as shown in Fig. 1. It consists of triple cavities, slots, windows, and holes. The thickness of each plate was 5 mm except the front-side one (2 mm). In order to characterize coupling effects for the vehicle, the cavity1 had three slots at front-side and the cavity2 had 5 windows.

A z -polarized external plane-wave that is incident from the front side of the model is coupled to the slots that located on the front side of the cavity1, and front window on the cavity2. The fields by these paths coupled to each cavity through the

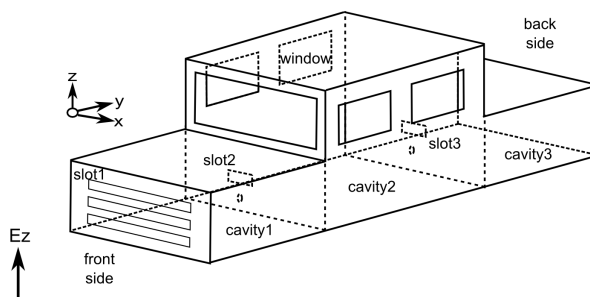


Fig. 1. Multiple cavity model of the simplified vehicle.

slot2 and slot3.

The coupled fields through the slots and windows build resonances inside the cavities. The shielding effectiveness ($SE = 20 \log_{10}(E_{inc}/E_i)$, where E_{inc} = incident electric field, E_i = internal electric field) was used as a measure of the resonances.

A. EMT Analysis of the Multiple Cavities

The general EM topology model is shown in Fig. 2. EM topology has been used to analyze the electromagnetic field coupling problem in large target such as aircraft [8]. Furthermore, it is useful method to analyze for complex system. Fundamentally, EM topology exploits the following:

1. Dividing the entire target into a set of sub-volumes according to characteristics of the model
2. Characterizing those sub-volumes assigning a proper governing equation
3. Constructing an equivalent topology and solving it using suitable equations

EM topology model is composed of junctions and tubes. The junctions correspond to port terminal devices such as resistors, inductors and capacitors, where voltages and currents can be evaluated. Usually, the junctions are placed at the boundaries of topology having different electromagnetic characteristics. The tubes are paths where the EM wave is transmitted between junctions, of which characteristics are determined by their material such as free space, microstrip line and coaxial cable. In Fig. 2, $W_i(0)$ and $W_k(L_n)$ are a reflected wave and an incident one at the junction, J_i respectively L_n is the length of the tube T_n , which means the propagation distance between the junction J_i and the junction J_k .

The simplified model of the vehicle shown in Fig. 1 can be represented by EM topology in Fig. 3. In Fig. 3, Apertures mean slots and windows of the vehicle. Sources of the EM topology denote the incident wave from outside of the model. The points that are desired to analyze inside the vehicle model are represented by observation points.

Based on EM topology shown in Fig. 3, the equations over aperture boundaries can be written as

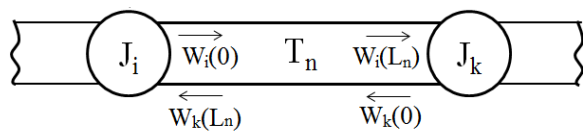


Fig. 2. General EM topology model.

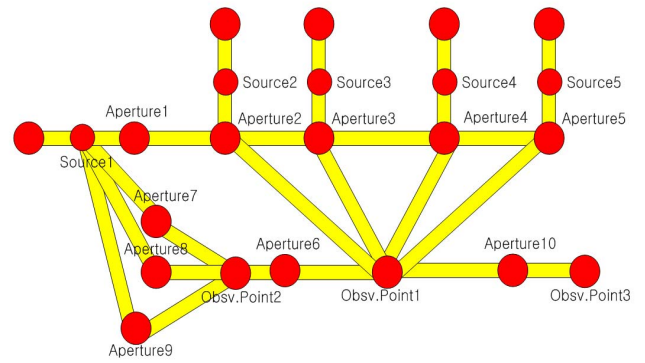


Fig. 3. EM topology model of simplified vehicle..

$$\left(H_x^{inc, FW} + H_x^{II, FW} \right) \Big|_{y=FW} = \left(H_x^{I(y=FW, y=slot2)} + H_x^{I(x=LSW)} + H_x^{I(x=RSW)} + H_x^{I(y=slot3)} \right) \Big|_{y=FW} \quad (1)$$

$$\left(H_x^{inc, FW} e^{+jk_{cav1}} + H_x^{II, slot1} \right) \Big|_{z=slot1} = \left(H_x^{I(y=slot1)} + H_x^{I(y=slot2)} \right) \Big|_{z=slot1} \quad (2)$$

$$\left(H_x^{I(y=FW, y=slot2)} + H_x^{I(x=LSW)} + H_x^{I(x=RSW)} + H_x^{I(y=slot3)} \right) \Big|_{y=slot2} = \left(H_x^{I(y=slot1)} + H_x^{I(y=slot2)} \right) \Big|_{y=slot2} \quad (3)$$

$$\left(H_y^{II, LSW} \right) \Big|_{x=LSW} = \left(H_y^{I(y=FW, y=slot2)} + H_y^{I(x=LSW)} + H_y^{I(x=RSW)} + H_y^{I(y=slot3)} \right) \Big|_{x=LSW} \quad (4)$$

$$\left(H_y^{II, RSW} \right) \Big|_{x=RSW} = \left(H_y^{I(y=FW, y=slot2)} + H_y^{I(x=LSW)} + H_y^{I(x=RSW)} + H_y^{I(y=slot3)} \right) \Big|_{x=RSW} \quad (5)$$

$$\left(H_x^{I(y=FW, y=slot2)} + H_x^{I(x=LSW)} + H_x^{I(x=RSW)} + H_x^{I(y=slot3)} \right) \Big|_{y=slot3} = H_x^{I(y=slot3)} \Big|_{y=slot3} \quad (6)$$

In equation (1)~(6), FW, LSW and RSW mean front window, left side windows and right side windows, respectively. Symbol I and II denote outside region and inside region of the cavity.

The unknowns of each aperture field are given from equation (1) to (6). The E-fields inside the vehicle model are then obtained from the unknowns.

B. Experimental Results of Electro-optical System

The EO measurement system that measures the shielding effectiveness of the multiple cavities is shown in Fig. 3. The field generation system and the cavities was located in a semi-anechoic chamber with dimensions of 6 m x 8 m x 3 m. A linearly polarized double ridged horn antenna generated an electric field to the cavities, and to compensate the drift of the amplifier the output of the amplifier was monitored by a power sensor.

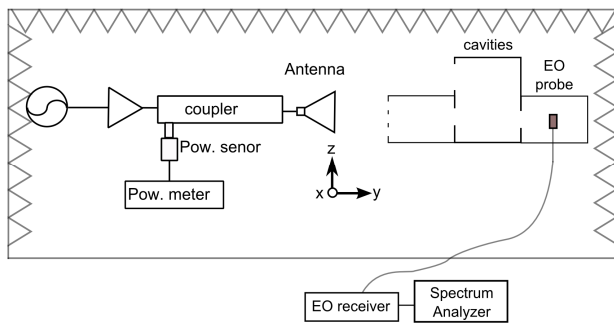


Fig. 3. Experimental setup of an EO measurement system with a semi-anechoic chamber.

A piece of LiTaO₃ with dimensions of 0.5 mm x 1.5 mm x 1.5 mm was used as the EO crystal. The crystal was supported by a ferrule and this crystal performed as a one axis E -field sensor along its optic-axis. An optical fiber was connected to the EO receiver located outside of the chamber. The receiver system consisted of a 1550 nm DFB laser with a TEC controller, an optical polarization controller, a circulator, and a photo-detector, which constructs an all-fiber optic link. The output of the receiver was monitored by a spectrum analyzer. The detailed configuration of the sensor and receiver system can be found in [2].

The reference output of E_{inc} was measured by the EO sensor without the cavities. The sensor axis was aligned to the incident z -polarized E -fields. To measure the internal fields, the cavity was placed in front of the antenna and the sensor was installed inside the center position of the cavity3. The internal electric field E_i was measured by the receiver and spectrum analyzer.

In Fig. 4 and 5, E_z and E_y fields were compared to the full wave 3D numerical simulation results and the simulation showed almost no component of x polarized field. The measurement result of the E_z field by the EO system shows a dominant resonance (TM₁₁₀ mode at 1.387 GHz), and secondary resonance (TM₁₂₀ mode at 2.291 GHz). The TM₁₀₁ mode resonance of the E_y field could be seen at 1.754 GHz.

ACKNOWLEDGEMENTS

This work was supported by the Korea Research Institute of Standards and Science under the project 'Development of Technologies for Next-Generation Electromagnetic Wave Measurement Standards' grant 14011004.

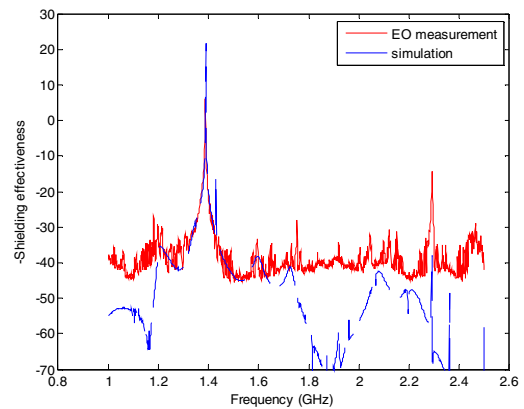


Fig. 4. Measurement result of the electric field (E_z) at center position of the cavity3.

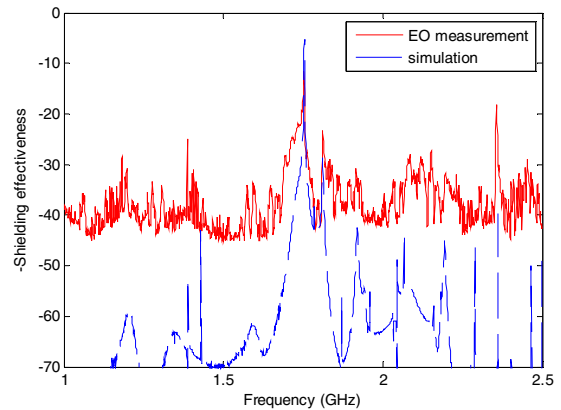


Fig. 5. Measurement result of the electric field (E_y) at center position of the cavity3.

REFERENCES

- [1] M. Backstrom, "HPM testing of a car: a representative example of the susceptibility of civil systems," *Proc. 13th Int. Zurich Symp. And Technical Exhibition on EMC*, 1999, pp. 189-190
- [2] J. LoVerti, A. Wilbers and A. Zwamborn, "Microwave interaction with a personal computer: experiment and modeling," *Proc. 13th Int. Zurich Symp. And Technical Exhibition on EMC*, 1999, pp. 203-206
- [3] C. E. Baum, T. K. Liu, and F. M. Tesche, *On the Analysis of General Multiconductor Transmission-line Networks*, Interaction Notes 350, November 1978.
- [4] F. M. Tesche, J. Keen, and C. M. Butler, Example of the Use of the BLT Equation for EM Field Propagation and Coupling Calculations, Interactions Notes 591, June 2004.
- [5] I. D. Flintoft, N. L. Whyman, J. F. Dawson and T. Konefal, "Fast and accurate intermediate-level modeling approach for EMC analysis of enclosures", *IEEE Proc. Sci. Meas. Technol.*, vol 149, pp. 281-285, 2002.
- [6] D.-J. Lee, J.-Y. Kwon, N.-W. Kang, and J. F. Whitaker, "Calibrated 100-dB-dynamic-range electro-optic probe for high-power microwave applications," *Opt. Express*, vol. 19, no. 15, pp. 14437-14450, Jul. 2011.
- [7] D.-J. Lee, C.-H. Cho, J.-W. Shin, and N.-W. Kang, "Photonic-assisted diagnosis of electromagnetic coupling into a generic object," *Meas. Sci. and Technol.*, vol. 24, no. 12, p. 125207, Dec. 2013.
- [8] Parmantier, J-P, "First Realistic Simulation of Effects of EM Coupling in Commercial Aircraft Wiring," *IEEE Computing & Control Engineering Journal*, April 1998.